4

ANTHROPOMETRY

4.0 SCOPE OF ANTHROPOMETRY IN MOVEMENT BIOMECHANICS

Anthropometry is the major branch of anthropology that studies the physical measurements of the human body to determine differences in individuals and groups. A wide variety of physical measurements are required to describe and differentiate the characteristics of race, sex, age, and body type. In the past, the major emphasis of these studies has been evolutionary and historical. However, more recently a major impetus has come from the needs of technological developments, especially man-machine interfaces: workspace design, cockpits, pressure suits, armor, and so on. Most of these needs are satisfied by basic linear, area, and volume measures. However, human movement analysis requires kinetic measures as well: masses, moments of inertia, and their locations. There exists also a moderate body of knowledge regarding the joint centers of rotation, the origin and insertion of muscles, the angles of pull of tendons, and the length and cross-sectional area of muscles.

4.0.1 Segment Dimensions

The most basic body dimension is the length of the segments between each joint. These vary with body build, sex, and racial origin. Dempster and coworkers (1955, 1959) have summarized estimates of segment lengths and joint center locations relative to anatomical landmarks. An average set of

 ISBN: 978-0-470-39818-0

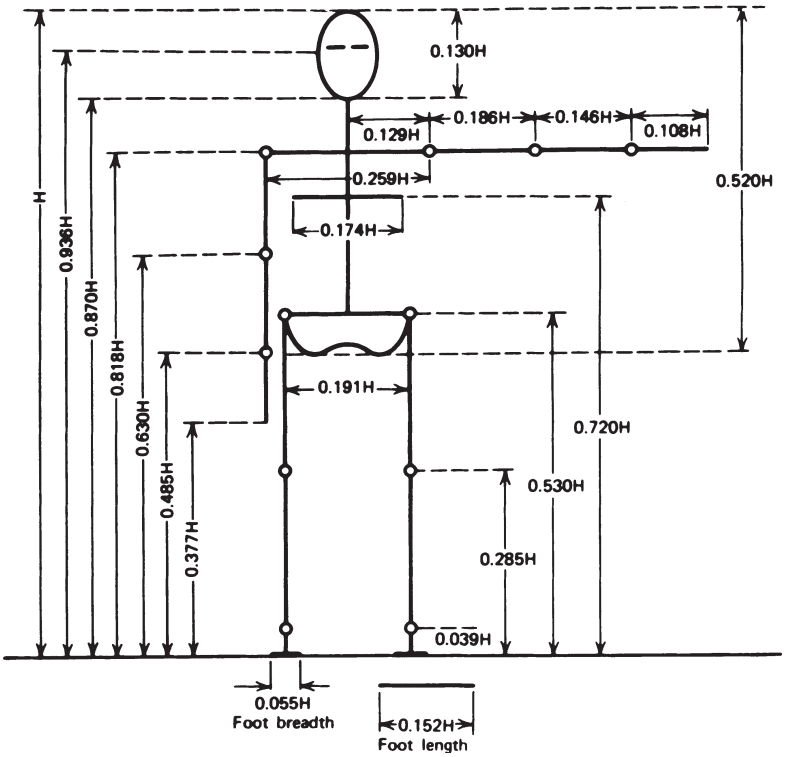

Figure 4.1 Body segment lengths expressed as a fraction of body height H.

segment lengths expressed as a percentage of body height was prepared by Drillis and Contini (1966) and is shown in Figure 4.1. These segment proportions serve as a good approximation in the absence of better data, preferably measured directly from the individual.

4.1 DENSITY, MASS, AND INERTIAL PROPERTIES

Kinematic and kinetic analyses require data regarding mass distributions, mass centers, moments of inertia, and the like. Some of these measures have been determined directly from cadavers; others have utilized measured segment volumes in conjunction with density tables, and more modern techniques use scanning systems that produce the cross-sectional image at many intervals across the segment.

4.1.1 Whole-Body Density

The human body consists of many types of tissue, each with a different density. Cortical bone has a specific gravity greater than 1.8, muscle tissue

is just over 1.0, fat is less than 1.0, and the lungs contain light respiratory gases. The average density is a function of body build, called *somatotype.* Drillis and Contini (1966) developed an expression for body density d as a function of ponderal index $c = h/w^{1/3}$, where w is body weight (pounds) and h is body height (inches):

$$d = 0.69 + 0.0297c \text{ kg/l} \tag{4.1}$$

The equivalent expression in metric units, where body mass is expressed in kilograms and height in meters, is:

$$d = 0.69 + 0.9c \text{ kg/l} \tag{4.2}$$

It can be seen that a short fat person has a lower ponderal index than a tall skinny person and, therefore, has a lower body density.

Example 4.1. Using Equations (4.1) and (4.2), calculate the whole-body density of an adult whose height is 5′10″ and who weighs 170 lb,

$$c = h/w^{1/3} = 70/170^{1/3} = 12.64$$

Using Equation (4.1),

$$d = 0.69 + 0.0297c = 0.69 + 0.0297 \times 12.64 = 1.065 \text{ kg/l}$$

In metric units,

$$h = 70/39.4 = 1.78 \text{ m}, \quad w = 170/2.2 = 77.3 \text{ kg}, \quad \text{and}$$
$$c = 1.78/77.3^{1/3} = 0.418$$

Using Equation (4.2),

$$d = 0.69 + 0.9c = 0.69 + 0.9 \times 0.418 = 1.066 \text{ kg/l}$$

4.1.2 Segment Densities

Each body segment has a unique combination of bone, muscle, fat, and other tissue, and the density within a given segment is not uniform. Generally, because of the higher proportion of bone, the density of distal segments is greater than that of proximal segments, and individual segments increase their densities as the average body density increases. Figure 4.2 shows these trends for six limb segments as a function of whole-body density, as calculated by Equations (4.1) or (4.2) or as measured directly (Drillis and Contini, 1966; Contini, 1972).

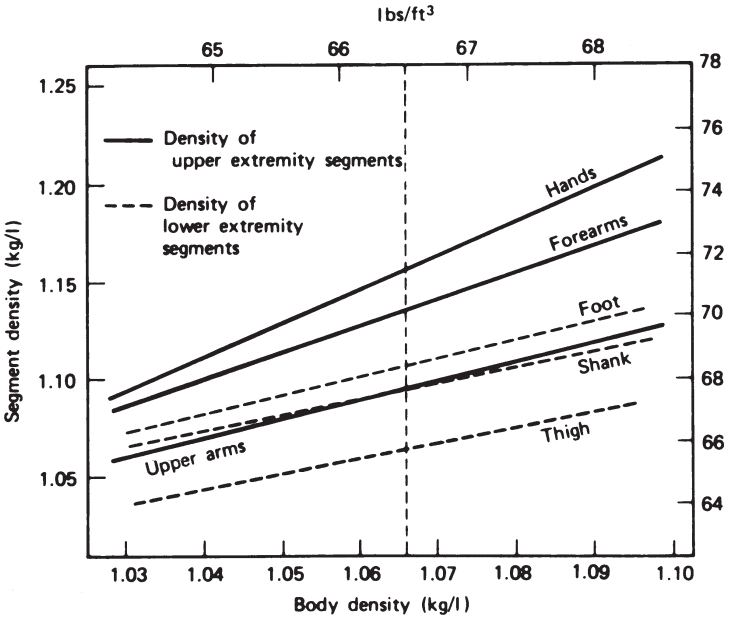

Figure 4.2 Density of limb segments as a function of average body density.

4.1.3 Segment Mass and Center of Mass

The terms *center of mass* and *center of gravity* are often used interchangeably. The more general term is center of mass, while the center of gravity refers to the center of mass in one axis only, that defined by the direction of gravity. In the two horizontal axes, the term center of mass must be used.

As the total body mass increases, so does the mass of each individual segment. Therefore, it is possible to express the mass of each segment as a percentage of the total body mass. Table 4.1 summarizes the compiled results of several investigators. These values are utilized throughout this text in subsequent kinetic and energy calculations. The location of the center of mass is also given as a percentage of the segment length from either the distal or the proximal end. In cadaver studies, it is quite simple to locate the center of mass by simply determining the center of balance of each segment. To calculate the center of mass in vivo, we need the profile of cross-sectional area and length. Figure 4.3 gives a hypothetical profile where the segment is broken into n sections, each with its mass indicated. The total mass M of the segment is:

$$M = \sum_{i=1}^{n} m_i \tag{4.3}$$

where m_i, is the mass of the ith section.

TABLE 4.1 Anthropometric Data

Segment	Definition	Segment Weight/Total Body Weight	Center of Mass/ Segment Length		Radius of Gyration/ Segment Length			Density
			Proximal	Distal	C of G Proximal		Distal	
Hand	Wrist axis/knuckle II middle finger	0.006 M	0.506	0.494 P	0.297	0.587	0.577 M	1.16
Forearm	Elbow axis/ulnar styloid	0.016 M	0.430	0.570 P	0.303	0.526	0.647 M	1.13
Upper arm	Glenohumeral axis/elbow axis	0.028 M	0.436	0.564 P	0.322	0.542	0.645 M	1.07
Forearm and hand	Elbow axis/ulnar styloid	0.022 M	0.682	0.318 P	0.468	0.827	0.565 P	1.14
Total arm	Glenohumeral joint/ulnar styloid	0.050 M	0.530	0.470 P	0.368	0.645	0.596 P	1.11
Foot	Lateral malleolus/head metatarsal II	0.0145 M	0.50	0.50 P	0.475	0.690	0.690 P	1.10
Leg	Femoral condyles/medial malleolus	0.0465 M	0.433	0.567 P	0.302	0.528	0.643 M	1.09
Thigh	Greater trochanter/femoral condyles	0.100 M	0.433	0.567 P	0.323	0.540	0.653 M	1.05
Foot and leg	Femoral condyles/medial malleolus	0.061 M	0.606	0.394 P	0.416	0.735	0.572 P	1.09
Total leg	Greater trochanter/medial malleolus	0.161 M	0.447	0.553 P	0.326	0.560	0.650 P	1.06
Head and neck	C7–T1 and 1st rib/ear canal	0.081 M	1.000	— PC	0.495	0.116	— PC	1.11
Shoulder mass	Sternoclavicular joint/glenohumeral axis	—	0.712	0.288	—	—	—	1.04
Thorax	C7–T1/T12–L1 and diaphragm*	0.216 PC	0.82	0.18	—	—	—	0.92
Abdomen	T12–L1/L4–L5*	0.139 LC	0.44	0.56	—	—	—	—
Pelvis	L4–L5/greater trochanter*	0.142 LC	0.105	0.895	—	—	—	—
Thorax and abdomen	C7–T1/L4–L5*	0.355 LC	0.63	0.37	—	—	—	—
Abdomen and pelvis	T12–L1/greater trochanter*	0.281 PC	0.27	0.73	—	—	—	1.01
Trunk	Greater trochanter/glenohumeral joint*	0.497 M	0.50	0.50	—	—	—	1.03
Trunk head neck	Greater trochanter/glenohumeral joint*	0.578 MC	0.66	0.34 P	0.503	0.830	0.607 M	—
Head, arms, and trunk (HAT)	Greater trochanter/glenohumeral joint*	0.678 MC	0.626	0.374 PC	0.496	0.798	0.621 PC	—
HAT	Greater trochanter/mid rib	0.678	1.142	—	0.903	1.456	—	—

*NOTE: These segments are presented relative to the length between the greater trochanter and the glenohumeral joint.

Source Codes: M, Dempster via Miller and Nelson; *Biomechanics of Sport*, Lea and Febiger, Philadelphia, 1973. P, Dempster via Plagenhoef; *Patterns of Human Motion*, Prentice-Hall, Inc. Englewood Cliffs, NJ, 1971. L, Dempster via Plagenhoef from living subjects; *Patterns of Human Motion*, Prentice-Hall, Inc., Englewood Cliffs, NJ, 1971. C, Calculated.

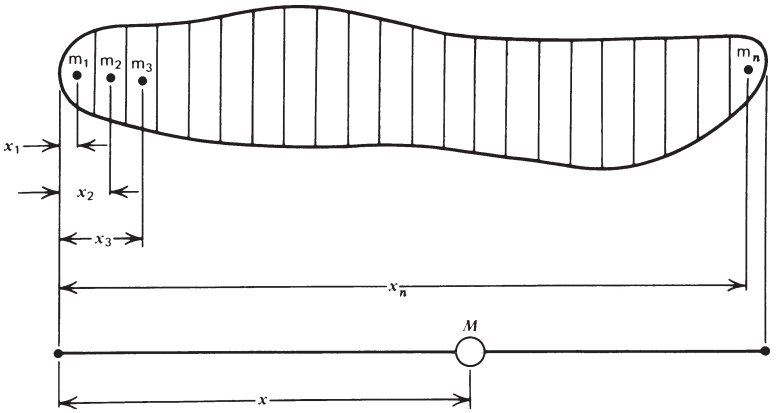

Figure 4.3 Location of the center of mass of a body segment relative to the distributed mass.

$$m_i = d_i V_i$$

where d_i = density of ith section
V_i = volume of ith section

If the density d is assumed to be uniform over the segment, then $m_i = dV_i$ and:

$$M = d \sum_{i=1}^{n} V_i \tag{4.4}$$

The center of mass is such that it must create the same net gravitational moment of force about any point along the segment axis as did the original distributed mass. Consider the center of mass to be located a distance x from the left edge of the segment,

$$Mx = \sum_{i=1}^{n} m_i x_i$$

$$x = \frac{1}{M} \sum_{i=1}^{n} m_i x_i \tag{4.5}$$

We can now represent the complex distributed mass by a single mass M located at a distance x from one end of the segment.

Example 4.2. From the anthropometric data in Table 4.1 calculate the coordinates of the center of mass of the foot and the thigh given the following

coordinates: ankle (84.9, 11.0), metatarsal (101.1, 1.3), greater trochanter (72.1, 92.8), and lateral femoral condyle (86.4, 54.9). From Table 4.1, the foot center of mass is 0.5 of the distance from the lateral malleolus (ankle) to the metatarsal marker. Thus, the center of mass of the foot is:

$$x = (84.9 + 101.1) \div 2 = 93.0 \text{ cm}$$
$$y = (11.0 + 1.3) \div 2 = 6.15 \text{ cm}$$

The thigh center of mass is 0.433 from the proximal end of the segment. Thus, the center of mass of the thigh is:

$$x = 72.1 + 0.433(86.4 - 72.1) = 78.3 \text{ cm}$$
$$y = 92.8 - 0.433(92.8 - 54.9) = 76.4 \text{ cm}$$

4.1.4 Center of Mass of a Multisegment System

With each body segment in motion, the center of mass of the total body is continuously changing with time. It is, therefore, necessary to recalculate it after each interval of time, and this requires knowledge of the trajectories of the center of mass of each body segment. Consider at a particular point in time a three-segment system with the centers of mass as indicated in Figure 4.4. The center of mass of the total system is located at (x_0, y_0), and each of these coordinates can be calculated separately; $M = m_1 + m_2 + m_3$, and:

$$x_0 = \frac{m_1x_1 + m_2x_2 + m_3x_3}{M} \tag{4.6}$$

$$y_0 = \frac{m_1y_1 + m_2y_2 + m_3y_3}{M} \tag{4.7}$$

The center of mass of the total body is a frequently calculated variable. Its usefulness in the assessment of human movement, however, is quite limited. Some researchers have used the time history center of mass to calculate the energy changes of the total body. Such a calculation is erroneous, because the center of mass does not account for energy changes related to reciprocal movements of the limb segments. Thus, the energy changes associated with the forward movement of one leg and the backward movement of another will not be detected in the center of mass, which may remain relatively unchanged. More about this will be said in Chapter 6. The major use of the body center of mass is in the analysis of sporting events, especially jumping events, where the path of the center of mass is critical to the success of the event because its trajectory is decided immediately at takeoff. Also, in studies of body posture and balance, the center of mass is an essential calculation.

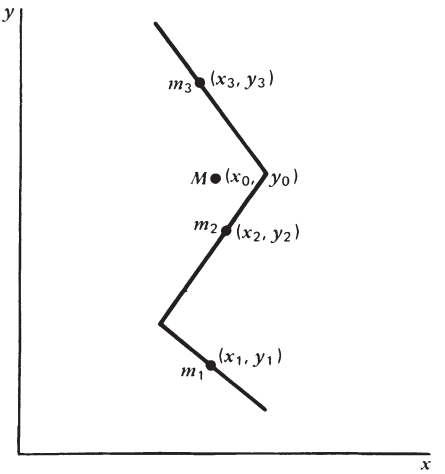

Figure 4.4 Center of mass of a three-segment system relative to the centers of mass of the individual segments.

4.1.5 Mass Moment of Inertia and Radius of Gyration

The location of the center of mass of each segment is needed for an analysis of translational movement through space. If accelerations are involved, we need to know the inertial resistance to such movements. In the linear sense, $F = ma$ describes the relationship between a linear force F and the resultant linear acceleration a. In the rotational sense, $M = I\alpha$. M is the moment of force causing the angular acceleration α. Thus, I is the constant of proportionality that measures the ability of the segment to resist changes in angular velocity. M has units of $\mathrm{N} \cdot \mathrm{m}$, α is in $\mathrm{rad/s^2}$, and I is in $\mathrm{kg} \cdot \mathrm{m^2}$. The value of I depends on the point about which the rotation is taking place and is a minimum when the rotation takes place about its center of mass. Consider a distributed mass segment as in Figure 4.3. The moment of inertia about the left end is:

$$\begin{aligned} I &= m_1 x_1^2 + m_2 x_2^2 + \cdots + m_n x_n^2 \\ &= \sum_{i=1}^{n} m_i x_i^2 \end{aligned} \tag{4.8}$$

It can be seen that the mass close to the center of rotation has very little influence on I, while the furthest mass has a considerable effect. This principle is used in industry to regulate the speed of rotating machines: the mass of a flywheel is concentrated at the perimeter of the wheel with as large a radius as possible. Its large moment of inertia resists changes in velocity and, therefore, tends to keep the machine speed constant.

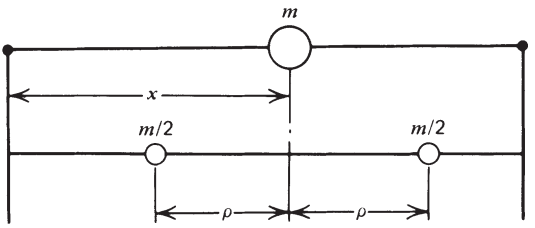

Figure 4.5 Radius of gyration of a limb segment relative to the location of the center of mass of the original system.

Consider the moment of inertia I_0 about the center of mass. In Figure 4.5 the mass has been broken into two equal point masses. The location of these two equal components is at a distance ρ_0 from the center such that:

$$I_0 = m\rho_0^2 \tag{4.9}$$

ρ_0 is the radius of gyration and is such that the two equal masses shown in Figure 4.5 have the same moment of inertia in the plane of rotation about the center of mass as the original distributed segment did. Note that the center of mass of these two equal point masses is still the same as the original single mass.

4.1.6 Parallel-Axis Theorem

Most body segments do not rotate about their mass center but rather about the joint at either end. In vivo measures of the moment of inertia can only be taken about a joint center. The relationship between this moment of inertia and that about the center of mass is given by the parallel-axis theorem. A short proof is now given.

$$\begin{aligned} I &= \frac{m}{2}(x - \rho_0)^2 + \frac{m}{2}(x + \rho_0)^2 \\ &= m\rho_0^2 + mx^2 \\ &= I_0 + mx^2 \end{aligned} \tag{4.10}$$

where I_0 = moment of inertia about center of mass
x = distance between center of mass and center of rotation
m = mass of segment

Actually, x can be any distance in either direction from the center of mass as long as it lies along the same axis as I_0 was calculated on.

Example 4.3. (a) A prosthetic leg has a mass of 3 kg and a center of mass of 20 cm from the knee joint. The radius of gyration is 14.1 cm. Calculate I about the knee joint.

$$I_0 = m\rho_0^2 = 3\,(0.141)^2 = 0.06 \text{ kg} \cdot \text{m}^2$$
$$I = I_0 + mx^2$$
$$= 0.06 + 3(0.2)^2 = 0.18 \text{ kg} \cdot \text{m}^2$$

(b) If the distance between the knee and hip joints is 42 cm, calculate I_h for this prothesis about the hip joint as the amputee swings through with a locked knee.

$$x = \text{distance from mass center to hip} = 20 + 42 = 62 \text{ cm}$$
$$I = I_0 + mx^2$$
$$= 0.06 + 3(0.62)^2 = 1.21 \text{ kg} \cdot \text{m}^2$$

Note that I_h is about 20 times that calculated about the center of mass.

4.1.7 Use of Anthropometric Tables and Kinematic Data

Using Table 4.1 in conjunction with kinematic data we can calculate many variables needed for kinetic energy analyses (see Chapters 5 and 6).This table gives the segment mass as a fraction of body mass and centers of mass as a fraction of their lengths from either the proximal or the distal end. The radius of gyration is also expressed as a fraction of the segment length about the center of mass, the proximal end, and the distal end.

4.1.7.1 Calculation of Segment Masses and Centers of Mass

Example 4.4. Calculate the mass of the foot, shank, thigh, and HAT and its location from the proximal or distal end, assuming that the body mass of the subject is 80 kg. Using the mass fractions for each segment,

$$\text{Mass of foot} = 0.0145 \times 80 = 1.16 \text{ kg}$$
$$\text{Mass of leg} = 0.0465 \times 80 = 3.72 \text{ kg}$$
$$\text{Mass of thigh} = 0.10 \times 80 = 8.0 \text{ kg}$$
$$\text{Mass of HAT} = 0.678 \times 80 = 54.24 \text{ kg}$$

Direct measures yielded the following segment lengths: foot = 0.195 m, leg = 0.435 m, thigh = 0.410 m, HAT = 0.295 m.

$$\begin{aligned}
\text{COM of foot} &= 0.50 \times 0.195 &&= 0.098 \text{ m between ankle and metatarsal markers} \\
\text{COM of leg} &= 0.433 \times 0.435 &&= 0.188 \text{ m below femoral condyle marker} \\
\text{COM of thigh} &= 0.433 \times 0.410 &&= 0.178 \text{ m below greater trochanter marker} \\
\text{COM of HAT} &= 1.142 \times 0.295 &&= 0.337 \text{ m above greater trochanter marker}
\end{aligned}$$

where COM stands for center of mass.

4.1.7.2 Calculation of Total-Body Center of Mass. The calculation of the center of mass of the total body is a special case of Equations (4.6) and (4.7). For an n-segment body system, the center of mass in the X direction is:

$$x = \frac{m_1x_1 + m_2x_2 + \cdots + m_nx_n}{m_1 + m_2 + \cdots + m_n} \tag{4.11}$$

where $m_1 + m_2 + \cdots + m_n = M$, the total body mass.

It is quite normal to know the values of $m_1 = f_1M, m_2 = f_2M$, and so on. Therefore,

$$x = \frac{f_1Mx_1 + f_2Mx_2 + \cdots + f_nMx_n}{M} = f_1x_1 + f_2x_2 + \cdots + f_nx_n \tag{4.12}$$

This equation is easier to use because all we require is knowledge of the fraction of total body mass and the coordinates of each segment's center of mass. These fractions are given in Table 4.1.

It is not always possible to measure the center of mass of every segment, especially if it is not in full view of the camera. In the sample data that follows, we have the kinematics of the right side of HAT and the right limb

TABLE 4.2 Coordinates for Body Segments, Example 4.5

	X (meters)		Y (meters)	
Segment	Right	Left	Right	Left
Foot	0.791	$1.353 - 0.707 = 0.646$	0.101	0.067
Leg	0.814	$1.355 - 0.707 = 0.648$	0.374	0.334
Thigh	0.787	$1.402 - 0.707 = 0.695$	0.708	0.691
½ HAT	0.721	$1.424 - 0.707 = 0.717$	1.124	1.122

$x = 0.0145(0.791 + 0.645) + 0.0465(0.814 + 0.648) + 0.1(0.787 + 0.695) + 0.339(0.721 + 0.717) = 0.724$ m

$y = 0.0145(0.101 + 0.067) + 0.0465(0.374 + 0.334) + 0.1(0.708 + 0.691) + 0.339(1.124 + 1.122) = 0.937$ m

during walking. It may be possible to simulate data for the left side of HAT and the left limb. If we assume symmetry of gait, we can say that the trajectory of the left limb is the same as that of the right limb, but out of phase by half a stride. Thus, if we use data for the right limb one-half stride later in time and shift them back in space one-half a stride length, we can simulate data for the left limb and left side of HAT.

Example 4.5. Calculate the total-body center of mass at a given frame 15. The time for one stride was 68 frames. Thus, the data from frame 15 become the data for the right lower limb and the right half of HAT, and the data one-half stride (34 frames) later become those for the left side of the body. All coordinates from frame 49 must now be shifted back in the x direction by a step length. An examination of the x coordinates of the heel during two successive periods of stance showed the stride length to be $264.2 - 122.8 = 141.4$ cm. Therefore, the step length is 70.7 cm = 0.707 m. Table 4.2 shows the coordinates of the body segments for both left and right halves of the body for frame 15. The mass fractions for each segment are as follows: foot = 0.0145, leg = 0.0465, thigh = 0.10, 1/2 HAT = 0.339. The mass of HAT dominates the body center of mass, but the energy changes in the lower limbs will be seen to be dominant as far as walking is concerned (see Chapter 6).

Center of mass (COM) analyses in three dimensions are not an easy measure to make because every segment of the body must be identified with markers and tracked with a three-dimensional (3D) imaging system. In some studies of standing, the horizontal anterior/posterior displacement of a rod attached to the pelvis has been taken as an estimate of center of mass movement (Horak et al., 1992). However, in situations when a patient flexes the total body at the hip (called a "hip strategy") to defend against a forward fall, the pelvis moves posteriorly considerably more than the center of mass (Horak and Nashner, 1986). In 3D assessments of COM displacements, the only technique is optical tracking of markers on all segments (or as many segments as possible). MacKinnon and Winter (1993) used a seven-segment total body estimate of the lower limbs and of the HAT to identify balance mechanisms in the frontal plane during level walking. Jian et al. (1993) reported a 3D analysis of a similar seven-segment estimate of the total body COM in conjunction with the center of pressure during initiation and termination of gait and identified the motor mechanisms responsible for that common movement.

The most complete measure of center of mass to date has been a 21-marker, 14-segment model that has been used to determine the mechanisms of balance during quiet standing (Winter et al., 1998). Figure 4.6 shows the location of the markers, and the accompanying table gives the definition of each of the 14 segments, along with mass fraction of each segment. It is worth

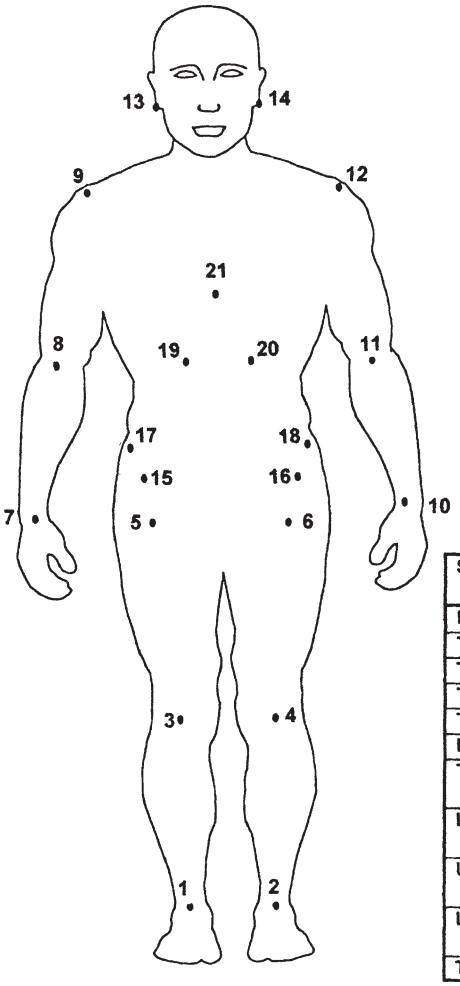

1. R Ankle
2. L Ankle
3. R Knee
4. L Knee
5. R Hip
6. L Hip
7. R Wrist
8. R Elbow
9. R Shoulder
10. L Wrist
11. L Elbow
12. L Shoulder
13. R Ear
14. L Ear
15. R ASIS
16. L ASIS
17. R Iliac Crest
18. L Iliac Crest
19. R Lower Rib
20. L Lower Rib
21. Xiphoid

Segment	Mass Fraction	Definition of Segment COM
Head	0.081	(13 + 14)/2
Trunk 4	0.136	(9 + 12 + 21)/3
Trunk 3	0.078	((19 +20)/2 + 21)/2
Trunk 2	0.065	(17 + 18 + 19 + 20)/4
Trunk 1	0.078	(17 + 18 + 15 + 16)/4
Pelvis	0.142	(15 + 16)/2
Thighs	0.100 (2)	0.433 x 3 + 0.567 x 5 and 0.433 x 4 + 0.567 x 6
Legs & feet	0.060 (2)	0.606 x 1 + 0.394 x 3 and 0.606 x 2 + 0.394 x 4
Upper arms	0.028 (2)	0.436 x 8 + 0.564 x 9 and 0.436 x 11 + 0.564 x 12
Lower arms	0.022 (2)	0.682 x 7 + 0.318 x 8 and 0.682 x 10 + 0.318 x 11
Total	1.00	

Figure 4.6 A 21-marker, 14-segment model to estimate the 3D center of mass of the total body in balance control experiments. Four trunk segments were necessary to track the internal mass shifts of the thoracic/lumbar volumes.

noting that most of the segments are fairly rigid segments (head, pelvis, upper and lower limbs). However, the trunk is not that rigid, and it required four separate segments to achieve a reliable estimate, mainly because these trunk segments undergo internal mass shifts due to respiratory and cardiac functions. The validity of any COM estimate can be checked with the equation for the inverted pendulum model during the movement: $\mathrm{COP} - \mathrm{COM} = -K \cdot \ddot{\mathrm{COM}}$ (Winter et al., 1998). COP is the center of pressure recorded from force plate data, $\ddot{\mathrm{COM}}$ is the horizontal acceleration of COM in either the

anterior/posterior or medial/lateral direction, and $K = I/Wh$, where I is the moment of inertia of the total body about the ankles, W is body weight, and h is the height of COM above the ankles.

4.1.7.3 Calculation of Moment of Inertia

Example 4.6. Calculate the moment of inertia of the leg about its center of mass, its distal end, and its proximal end. From Table 4.1, the mass of the leg is $0.0465 \times 80 = 3.72$ kg. The leg length is given as 0.435 m. The radius of gyration/segment length is 0.302 for the center of mass, 0.528 for the proximal end, and 0.643 for the distal end.

$$I_0 = 3.72(0.435 \times 0.302)^2 = 0.064 \text{ kg} \cdot \text{m}^2$$

About the proximal end,

$$I_p = 3.72(0.435 \times 0.528)^2 = 0.196 \text{ kg} \cdot \text{m}^2$$

About the distal end,

$$I_d = 3.72(0.435 \times 0.643)^2 = 0.291 \text{ kg} \cdot \text{m}^2$$

Note that the moment of inertia about either end could also have been calculated using the parallel-axis theorem. For example, the distance of the center of mass of the leg from the proximal end is $0.433 \times 0.435 = 0.188$ m, and:

$$I_p = I_0 + mx^2 = 0.064 + 3.72(0.188)^2 = 0.196 \text{ kg} \cdot \text{m}^2$$

Example 4.7. Calculate the moment of inertia of HAT about its proximal end and about its center of mass. From Table 4.1, the mass of HAT is $0.678 \times 80 = 54.24$ kg. The HAT length is given as 0.295 m. The radius of gyration about the proximal end/segment length is 1.456.

$$I_p = 54.24(0.295 \times 1.456)^2 = 10.01 \text{ kg} \cdot \text{m}^2$$

From Table 4.1, the center of mass/segment length = 1.142 from the proximal end.

$$I_0 = I_p - mx^2 = 10.01 - 54.24(0.295 \times 1.142)^2 = 3.85 \text{ kg} \cdot \text{m}^2$$

We could also use the radius of gyration/segment length about the center of mass = 0.903.

$$I_0 = mp^2 = 54.24(0.295 \times 0.903)^2 = 3.85 \text{ kg} \cdot \text{m}^2$$

4.2 DIRECT EXPERIMENTAL MEASURES

For more exact kinematic and kinetic calculations, it is preferable to have directly measured anthropometric values. The equipment and techniques that have been developed have limited capability and sometimes are not much of an improvement over the values obtained from tables.

4.2.1 Location of the Anatomical Center of Mass of the Body

The center of mass of the total body, called the *anatomical center of mass*, is readily measured using a balance board, as shown in Figure 4.7*a*. It consists of a rigid board mounted on a scale at one end and a pivot point at the other end, or at some convenient point on the other side of the body's center of mass. There is an advantage in locating the pivot as close as possible to the center of mass. A more sensitive scale (0–5 kg) rather than a 50- or 100-kg scale is possible, which will result in greater accuracy. It is presumed that the weight of the balance board, w_1, and its location, x_1, from the pivot are both known along with the body weight, w_2. With the body lying prone the scale reading is S (an upward force acting at a distance x_3 from the pivot). Taking moments about the pivot:

$$w_1x_1 + w_2x_2 = Sx_3$$

$$x_2 = \frac{Sx_3 - w_1x_1}{w_2} \tag{4.13}$$

4.2.2 Calculation of the Mass of a Distal Segment

The mass or weight of a distal segment can be determined by the technique demonstrated in Figure 4.7*b*. The desired segment, here the leg and foot, is lifted to a vertical position so that its center of mass lies over the joint center. Prior to lifting, the center of mass was x_4 from the pivot point, with the scale reading S. After lifting, the leg center of mass is x_5 from the pivot, and the scale reading has increased to S^1. The decrease in the clockwise moment due to the leg movement is equal to the increase in the scale reaction force moment about the pivot point,

$$W_4(x_4 - x_5) = (S^1 - S)x_3$$

$$w_4 = \frac{\left(S^1 - S\right)x_3}{(x_4 - x_5)} \tag{4.14}$$

The major error in this calculation is the result of errors in x_4, usually obtained from anthropometric tables. To get the mass of the total limb, this experiment can be repeated with the subject lying on his back and the limb flexed at an angle of 90°. From the mass of the total limb, we can now subtract that of the leg and foot to get the thigh mass.

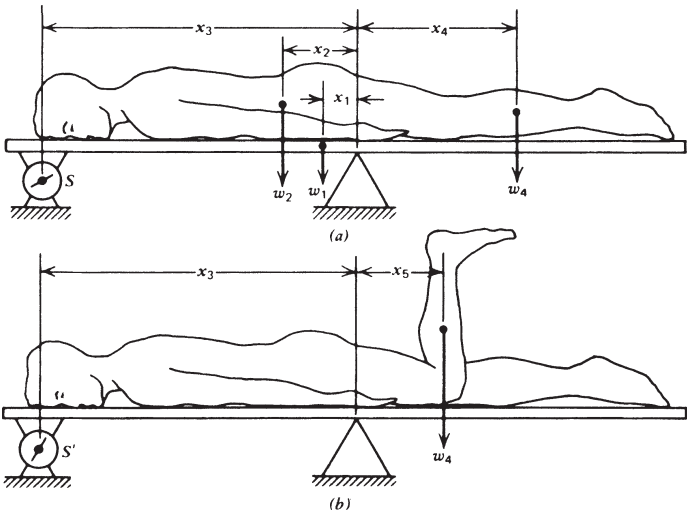

Figure 4.7 Balance board technique. (*a*) In vivo determination of mass of the location of the anatomical center of mass of the body. (*b*) Mass of a distal segment. See text for details.

4.2.3 Moment of Inertia of a Distal Segment

The equation for the moment of inertia, described in Section 4.1.5, can be used to calculate I at a given joint center of rotation. I is the constant of proportionality that relates the joint moment to the segment's angular acceleration, assuming that the proximal segment is fixed. A method called the *quick release experiment* can be used to calculate I directly and requires the arrangement pictured in Figure 4.8. We know that $I = M/\alpha$, so if we can measure the moment M that causes an angular acceleration α, we can calculate I directly. A horizontal force F pulls on a convenient rope or cable at a distance y_1 from the joint center and is restrained by an equal and opposite force acting on a release mechanism. An accelerometer is attached to the leg at a distance y_2 from the joint center. The tangential acceleration a is related to the angular acceleration of the leg α by $a = y_2\alpha$.

With the forces in balance as shown, the leg is held in a neutral position and no acceleration occurs. If the release mechanism is actuated, the restraining force suddenly drops to zero and the net moment acting on the leg is Fy_1, which causes an instantaneous acceleration α. F and a can be recorded on a dual-beam storage oscilloscope; most pen recorders have too low a frequency response to capture the acceleration impulse. The moment of inertia can now be calculated,

$$I = \frac{M}{\alpha} = \frac{Fy_1y_2}{a} \tag{4.15}$$

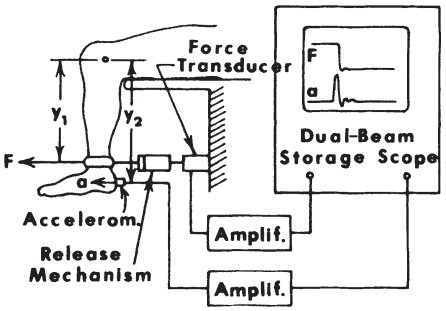

Figure 4.8 Quick-release technique for the determination of the mass moment of inertia of a distal segment. Force F applied horizontally results, after release of the segment, in an initial acceleration a. Moment of inertia can then be calculated from F, y_1, y_2.

Figure 4.8 shows the sudden burst of acceleration accompanied by a rapid decrease in the applied force F. This force drops after the peak of acceleration and does so because the forward displacement of the limb causes the tension to drop in the pulling cable. A convenient release mechanism can be achieved by suddenly cutting the cable or rope that holds back the leg. The sudden accelerometer burst can also be used to trigger the oscilloscope sweep so that the rapidly changing force and acceleration can be captured.

More sophisticated experiments have been devised to measure more than one parameter simultaneously. Such techniques were developed by Hatze (1975) and are capable of determining the moment of inertia, the location of the center of mass, and the damping coefficient simultaneously.

4.2.4 Joint Axes of Rotation

Markers attached to the body are usually placed to represent our best estimate of a joint center. However, because of anatomical constraints, our location can be somewhat in error. The lateral malleolus, for example, is a common location for ankle joint markers. However, the articulation of the tibial/talus surfaces is such that the distal end of the tibia (and the fibula) move in a small arc over the talus. The true axis of rotation is actually a few centimeters distal of the lateral malleolus. Even more drastic differences are evident at some other joints. The hip joint is often identified in the sagittal plane by a marker on the upper border of the greater trochanter. However, it is quite evident that the marker is somewhat more lateral than the center of the hip joint such that internal and external rotations of the thigh relative to the pelvis may cause considerable errors, as will abduction/adduction at that joint.

Thus, it is important that the true axes of rotation be identified relative to anatomical markers that we have placed on the skin. Several techniques have been developed to calculate the instantaneous axis of rotation of any joint based on the displacement histories of markers on the two adjacent

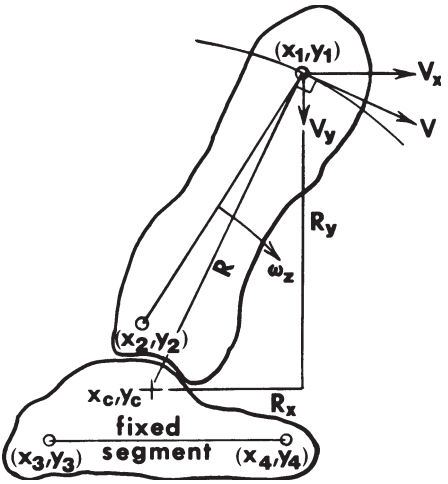

Figure 4.9 Technique used to calculate the axis of rotation between two adjacent segments x_c, y_c. Each segment must have two markers in the plane of movement. After data collection, the segments are rotated and translated so that one segment is fixed in space. Thus, the moving-segment kinematics reflects the relative movement between the two segments and the axis of rotation can be located relative to the anatomical location of markers on that fixed segment. See text for complete details.

segments. Figure 4.9 shows two segments in a planar movement. First, they must be translated and rotated in space so that one segment is fixed in space and the second rotates as shown. At any given instant in time, the true axis of rotation is at (x_c, y_c) within the fixed segment, and we are interested in the location of (x_c, y_c) relative to anatomical coordinates (x_3, y_3) and (x_4, y_4) of that segment. Markers (x_1, y_1) and (x_2, y_2) are located as shown; (x_1, y_1) has an instantaneous tangential velocity $\overline{V}$ and is located at a radius $\overline{R}$ from the axis of rotation. From the line joining (x_1, y_1) to (x_2, y_2), we calculate the angular velocity of the rotating segment $\overline{\omega}_z$. With one segment fixed in space, $\overline{\omega}_z$ is nothing more than the joint angular velocity,

$$\overline{V} = \overline{\omega}_z \times \overline{R} \tag{4.16a}$$

or, in Cartesian coordinates,

$$V_x \hat{i} + V_y \hat{j} = \left(R_y \omega_z\right) \hat{i} - \left(R_x \omega_z\right) \hat{j}$$

Therefore,

$$V_x = R_y \omega_z \quad \text{and} \quad V_y = -R_x \omega_z \tag{4.16b}$$

Since V_x, V_y, and ω_z can be calculated from the marker trajectory data, R_y and R_x can be determined. Since x_1, y_1 is known, the axis of rotation x_c, y_c

can be calculated. Care must be taken when ω_z approaches 0 or reverses its polarity, because R, as calculated by Equation (4.16a), becomes indeterminate or falsely approaches very large values. In practice, we have found errors become significant when ω_z falls below 0.5 r/s.

4.3 MUSCLE ANTHROPOMETRY

Before we can calculate the forces produced by individual muscles during normal movement, we usually need some dimensions from the muscles themselves. If muscles of the same group share the load, they probably do so proportionally to their relative cross-sectional areas. Also, the mechanical advantage of each muscle can be different, depending on the moment arm length at its origin and insertion, and on other structures beneath the muscle or tendon that alter the angle of pull of the tendon.

4.3.1 Cross-Sectional Area of Muscles

The functional or physiologic cross-sectional area (PCA) of a muscle is a measure of the number of sarcomeres in parallel with the angle of pull of the muscles. In pennate muscles, the fibers act at an angle from the long axis and, therefore, are not as effective as fibers in a parallel-fibered muscle. The angle between the long axis of the muscle and the fiber angle is called *pennation angle*. In parallel-fibered muscle, the PCA is:

$$\text{PCA} = \frac{m}{dl} \text{ cm}^2 \tag{4.17}$$

where m = mass of muscle fibers, grams
d = density of muscle, g/cm^3, = 1.056 g/cm^3
l = length of muscle fibers, centimeters

In pennate muscles, the physiological cross-sectional area becomes:

$$\text{PCA} = \frac{m \cos\theta}{dl} \text{ cm}^2 \tag{4.18}$$

where: θ is the pennation angle, which increases as the muscle shortens.

Wickiewicz et al. (1983), using data from three cadavers, measured muscle mass, fiber lengths, and pennation angle for 27 muscles of the lower extremity. Representative values are given in Table 4.3. The PCA as a percentage of the total cross-sectional area of all muscles crossing a given joint is presented in Table 4.4. In this way, the relative potential contribution of a group of agonist muscles can be determined, assuming that each is generating the same stress. Note that a double-joint muscle, such as the gastrocnemius, may represent different percentages at different joints because of the different total PCA of all muscles crossing each joint.

TABLE 4.3 Mass, Length, and PCA of Some Muscles

Muscle	Mass (g)	Fiber Length (cm)	PCA (cm^2)	Pennation Angle (deg)
Sartorius	75	38	1.9	0
Biceps femoris (long)	150	9	15.8	0
Semitendinosus	75	16	4.4	0
Soleus	215	3.0	58	30
Gastrocnemius	158	4.8	30	15
Tibialis posterior	55	2.4	21	15
Tibialis anterior	70	7.3	9.1	5
Rectus femoris	90	6.8	12.5	5
Vastus lateralis	210	6.7	30	5
Vastus medialis	200	7.2	26	5
Vastus intermedius	180	6.8	25	5

TABLE 4.4 Percent PCA of Muscles Crossing Ankle, Knee, and Hip Joints

Ankle		Knee		Hip	
Muscle	%PCA	Muscle	%PCA	Muscle	%PCA
Soleus	41	Gastrocnemius	19	Iliopsoas	9
Gastrocnemius	22	Biceps Femoris (small)	3	Sartorius	1
Flexor Hallucis Longus	6	Biceps Femoris (long)	7	Pectineus	1
Flexor Digitorum Longus	3	Semitendinosus	3	Rectus Femoris	7
Tibialis Posterior	10	Semimembranosus	10	Gluteus Maximus	16
Peroneus Brevis	9	Vastus Lateralis	20	Gluteus Medius	12
Tibialis Anterior	5	Vastus Medialis	15	Gluteus Minimus	6
Extensor Digitorum Longus	3	Vastus Intermedius	13	Adductor Magnus	11
Extensor Hallucis Longus	1	Rectus Femoris	8	Adductor Longus	3
		Sartorius	1	Adductor Brevis	3
		Gracilis	1	Tensor Fasciae Latae	1
				Biceps Femoris (long)	6
				Semitendinosus	3
				Semimembranosus	8
				Piriformis	2
				Lateral Rotators	13

4.3.2 Change in Muscle Length during Movement

A few studies have investigated the changes in the length of muscles as a function of the angles of the joints they cross. Grieve and colleagues (1978), in a study on eight cadavers, reported percentage length changes of the gastrocnemius muscle as a function of the knee and ankle angle. The resting length of the gastrocs was assumed to be when the knee was flexed 90° and the ankle was in an intermediate position, neither plantarflexed nor dorsiflexed. With 40° plantarflexion, the muscle shortened 8.5% and linearly changed its length to a 4% increase at 20° dorsiflexion. An almost linear curve described the changes at the knee: 6.5% at full extension to a 3% decrease at 150° flexion.

4.3.3 Force per Unit Cross-Sectional Area (Stress)

A wide range of stress values for skeletal muscles has been reported (Haxton, 1944; Alexander and Vernon, 1975; Maughan et al., 1983). Most of these stress values were measured during isometric conditions and range from 20 to 100 N/cm^2. These higher values were recorded in pennate muscles, which are those whose fibers lie at an angle from the main axis of the muscle. Such an orientation effectively increases the cross-sectional area above that measured and used in the stress calculation. Haxton (1944) related force to stress in two pennate muscles (gastrocs and soleus) and found stresses as high as 38 N/cm^2. Dynamic stresses have been calculated in the quadriceps during running and jumping to be about 70 N/cm^2 (based on a peak knee extensor moment of 210 $N \cdot m$ in adult males) and about 100 N/cm^2 in isometric maximum voluntary contractions (MVCs) (Maughan et al., 1983).

4.3.4 Mechanical Advantage of Muscle

The origin and insertion of each muscle defines the angle of pull of the tendon on the bone and, therefore, the mechanical leverage it has at the joint center. Each muscle has its unique moment arm length, which is the length of a line normal to the muscle passing through the joint center. This moment arm length changes with the joint angle. One of the few studies done in this area (Smidt, 1973) reports the average moment arm length (26 subjects) for the knee extensors and for the hamstrings acting at the knee. Both these muscle groups showed an increase in the moment length as the knee was flexed, reaching a peak at 45°, then decreasing again as flexion increased to 90°. Wilkie (1950) has also documented the moments and lengths for elbow flexors.

4.3.5 Multijoint Muscles

A large number of the muscles in the human body pass over more than one joint. In the lower limbs, the hamstrings are extensors of the hip and flexors

of the knee, the rectus femoris is a combined hip flexor and knee extensor, and the gastrocnemius are knee flexors and ankle plantarflexors. The fiber length of many of these muscles may be insufficient to allow a complete range of movement of both joints involved. Elftman (1966) has suggested that many normal movements require lengthening at one joint simultaneously with shortening at the other. Consider the action of the rectus femoris, for example, during early swing in running. This muscle shortens as a result of hip flexion and lengthens at the knee as the leg swings backward in preparation for swing. The tension in the rectus femoris simultaneously creates a flexor hip moment (positive work) and an extensor knee moment to decelerate the swinging leg (negative work) and start accelerating it forward. In this way, the net change in muscle length is reduced compared with two equivalent single-joint muscles, and excessive positive and negative work within the muscle can be reduced. A double-joint muscle could even be totally isometric in such situations and would effectively be transferring energy from the leg to the pelvis in the example just described. In running during the critical push-off phase, when the plantarflexors are generating energy at a high rate, the knee is continuing to extend. Thus, the gastrocnemii may be essentially isometric (they may appear to be shortening at the distal end and lengthening at the proximal end). Similarly, toward the end of swing in running, the knee is rapidly extending while the hip has reached full flexion and is beginning to reverse (i.e., it has an extensor velocity). Thus, the hamstrings appear to be rapidly lengthening at the distal end and shortening at the proximal end, with the net result that they may be lengthening at a slower rate than a single joint would.

It is also critical to understand the role of the major biarticulate muscles of the lower limb during stance phase of walking or running. Figure 4.10 shows the gastrocnemii, hamstrings, and rectus femoris and their moment-arm lengths at their respective proximal and distal ends. The hamstrings have a 5-cm moment-arm at the ankle and 3.5-cm moment-arm at the knee. Thus, when they are active during stance, their contribution to the ankle extensor moment is about 50% greater than their contribution to the knee flexor moment. The net effect of these two contributions is to cause the leg to rotate posteriorly and prevent the knee from collapsing. The hamstrings, with the exception of the short head of the biceps femoris, have moment-arms of 6–7 cm at the hip but only 3.5 cm at the knee. Thus, when these muscles are active during stance, their contribution to hip extension is about twice their contribution to knee flexion. The net effect of these two actions is to cause the thigh to rotate posteriorly and prevent the knee from collapsing. Finally, the rectus femoris is the only biarticulate muscle of the large quadriceps group, and its moment-arm at the hip is slightly larger than at the knee. However, the quadriceps activate as a group, and because the uniarticulate quadriceps comprise 84% of the PCA of the quadriceps (see Table 4.3), the dominant action is knee extension. Thus, the net effect of the major biarticulate muscles of the lower limb is extension at all three joints, and therefore they

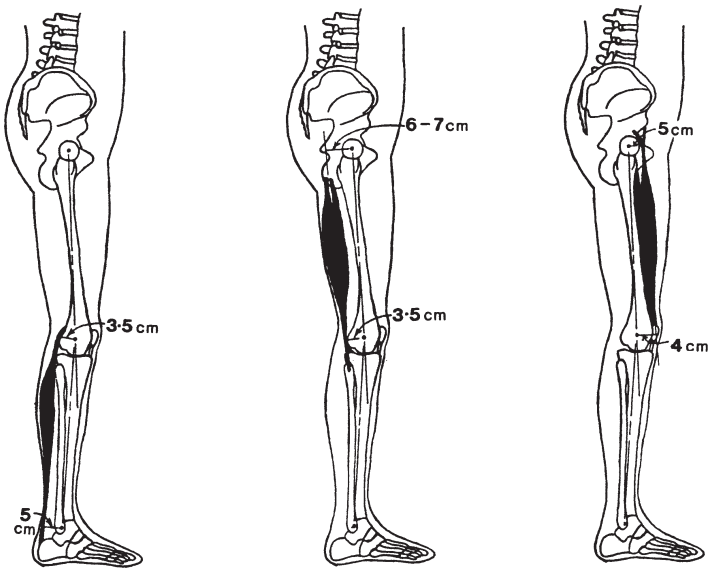

Figure 4.10 Three major biarticulate muscles of the lower limb. Shown are the gastrocnemii, hamstrings, and rectus femoris, and their moment-arm lengths at their proximal and distal ends. These moment-arms are critical to the functional role of these muscle groups during weight bearing; see the text for details.

contribute, along with all the uniarticulate extensors, to defending against a gravity-induced collapse. The algebraic summation of all three moments during stance phase of gait has been calculated and has been found to be dominantly extensor (Winter, 1984). This summation has been labeled the support moment and is discussed further in Section 5.2.6.

4.4 PROBLEMS BASED ON ANTHROPOMETRIC DATA

1. (a) Calculate the average body density of a young adult whose height is 1.68 m and whose mass is 68.5 kg. Answer: 1.059 kg/1.

(b) For the adult in (a), determine the density of the forearm and use it to estimate the mass of the forearm that measures 24.0 cm from the ulnar styloid to the elbow axis. Circumference measures (in cm) taken at 1-cm intervals starting at the wrist are 20.1, 20.3, 20.5, 20.7, 20.9, 21.2, 21.5, 21.9, 22.5, 23.2, 23.9, 24.6, 25.1, 25.7, 26.4, 27.0, 27.5, 27.9, 28.2, 28.4, 28.4, 28.3, 28.2, and 28.0. Assuming the forearm to have a circular cross-sectional area over its entire length, calculate the volume of the forearm and its mass. Compare the mass as calculated with that estimated using averaged anthropometric data (Table 4.1). *Answer:* Forearm density = 1.13 kg/1; volume = 1.174 1; mass = 1.33 kg. Mass calculated from Table 4.1 = 1.10 kg.

(c) Calculate the location of the center of mass of the forearm along its long axis and give its distance from the elbow axis. Compare that with the center of mass as determined from Table 4.1. *Answer:* COM = 10.34 cm from the elbow; from Table 4.1, COM = 10.32 cm from the elbow.

(d) Calculate the moment of inertia of the forearm about the elbow axis. Then calculate its radius of gyration about the elbow and compare it with the value calculated from Table 4.1 *Answer:* $I_p = 0.0201\,\text{kg} \cdot \text{m}^2$; radius of gyration = 12.27 cm; radius of gyration from Table 4.1 = 12.62 cm.

2. (a) From data listed in Table A.3 in Appendix A, calculate the center of mass of the lower limb for frame 70. *Answer:* $x = 1.755\,\text{m}$; $y = 0.522\,\text{m}$.

(b) Using your data of stride length (Problem 2(f) in Section 3.8) and a stride time of 68 frames, create an estimate (assuming symmetrical gait) of the coordinates of the left half of the body for frame 30. From the segment centers of mass (Table A.4), calculate the center of mass of the right half of the body (foot + leg + high + 1/2 HAT), and of the left half of the body (using segment data suitably shifted in time and space). Average the two centers of mass to get the center of mass of the total body for frame 30. *Answer:* $x\,1.025\,\text{m}, y = 0.904\,\text{m}$.

3. (a) Calculate the moment of inertia of the HAT about its center of mass for the subject described in Appendix A. Answer: $I_0 = 1.96\,\text{kg} \cdot \text{m}^2$.

(b) Assuming that the subject is standing erect with the two feet together, calculate the moment of inertia of HAT about the hip joint, the knee joint, and the ankle joint. What does the relative size of these moments of inertia tell us about the relative magnitude of the joint moments required to control the inertial load of HAT. *Answer:* $I_h = 5.09\,\text{kg} \cdot \text{m}^2, I_k = 15.78\,\text{kg} \cdot \text{m}^2, I_a = 42.31\,\text{kg} \cdot \text{m}^2$.

(c) Assuming that the center of mass of the head is 1.65 m from the ankle, what percentage does it contribute to the moment of inertia of HAT about the ankle? *Answer:* I_{head} about ankle $= 12.50\,\text{kg} \cdot \text{m}^2$, which is 29.6% of I_{hat} about the ankle.

4. (a) Calculate the moment of inertia of the lower limb of the subject in Appendix A about the hip joint. Assume that the knee is not flexed and the foot is a point mass located 6 cm distal to the ankle. *Answer:* $I_{\text{lower limb}}$ about hip $= 1.39\,\text{kg} \cdot \text{m}^2$.

(b) Calculate the increase in the moment of inertia as calculated in (a) when a ski boot is worn. The mass of the ski boot is 1.8 kg, and assume it to be a point mass located 1 cm distal to the ankle. *Answer:* I_{boot} about hip $= 1.01\,\text{kg} \cdot \text{m}^2$.

4.5 REFERENCES

Alexander, R. McN. and A. Vernon. "The Dimensions of Knee and Ankle Muscles and the Forces They Exert,'' *J. Human Movement Studies* **1**:115–123, 1975.

Contini, R. "Body Segment Parameters, Part II,'' *Artificial Limbs* **16**:1–19, 1972.

Dempster, W. T. "Space Requirements of the Seated Operator,'' WADC-TR-55-159, Wright Patterson Air Force Base, 1955.

Dempster, W. T., W. C. Gabel, and W. J. L. Felts. "The Anthropometry of Manual Work Space for the Seated Subjects,'' *Am. J. Phys. Anthrop.* **17**:289–317, 1959.

Drillis, R. and R. Contini. "Body Segment Parameters,'' Rep. 1163-03, Office of Vocational Rehabilitation, Department of Health, Education, and Welfare, New York, 1966.

Elftman, H. "Biomechanics of Muscle, with Particular Application to Studies of Gait,'' *J. Bone Joint Surg.* **48-A**: 363–377, 1966.

Grieve, D. W., P. R. Cavanagh, and S. Pheasant. "Prediction of Gastrocnemius Length from Knee and Ankle Joint Posture,'' *Biomechanics, Vol. VI-A*, E. Asmussen and K. Jorgensen, Eds. (University Park Press, Baltimore, MD, 1978), pp. 405–412.

Haxton, H. A. "Absolute Muscle Force in the Ankle Flexors of Man,'' *J. Physiol.* **103**:267–273, 1944.

Hatze, H. "A New Method for the Simultaneous Measurement of the Moment of Inertia, the Damping Coefficient and the Location of the Center of Mass of a Body Segment in situ,'' *Eur. J. Appl. Physiol.* **34**:217–266, 1975.

Horak, F. B. and L. M. Nashner. "Central Programming of Postural Movements: Adaptation to Altered Support Surface Configurations,'' *J. Neurophysiol.* **55**:1369–1381, 1986.

Horak, F. B., J. G. Nutt, and L. M. Nashner. "Postural Inflexibility in Parkinsonian Subjects,'' *J. Neurol. Sci.* **111**:46–58, 1992.

Jian, Y., D. A. Winter, M. G. Ishac, and L. Gilchrist. "Trajectory of the Body COG and COP During Initiation and Termination of Gait,'' *Gait and Posture* **1**:9–22, 1993.

MacKinnon, C. D. and D. A. Winter. "Control of Whole Body Balance and Posture in the Frontal Plane During Walking,'' *J. Biomech.* **26**:633–644, 1993.

Maughan, R. J., J. S. Watson, and J. Weir. "Strength and Cross-Sectional Area of Human Skeletal Muscle,'' *J. Physiol.* **338**:37–49, 1983.

Smidt, G. L. "Biomechanical Analysis of Knee Flexion and Extension,'' *J. Biomech.*, **6**:79–92, 1973.

Wickiewcz, T. L., R. R. Roy, P. L. Powell, and V. R., Edgerton. "Muscle Architecture of the Human Lower Limb," *Clin. Orthop. Rel. Res.* **179**:275–283, 1983.

Wilkie, D. R. "The Relation between Force and Velocity in Human Muscle,'' *J. Physiol.* **110**:249–280, 1950.

Winter, D. A. "Kinematic and Kinetic Patterns in Human Gait: Variability and Compensating Effects,'' *Hum. Movement Sci.* **3**:51–76, 1984.

Winter, D. A., A. E. Patla, F. Prince, M. G. Ishac, and K. Gielo-Perczak. "Stiffness Control of Balance in Quiet Standing,'' *J. Neurophysiol.* **80**:1211–1221, 1998.